

# Accurate determination of the free-free Gaunt factor I – non-relativistic Gaunt factors

P. A. M. van Hoof<sup>1\*</sup>, R. J. R. Williams<sup>2</sup>, K. Volk<sup>3</sup>, M. Chatzikos<sup>4</sup>, G. J. Ferland<sup>4</sup>,  
M. Lykins<sup>4</sup>, R. L. Porter<sup>5</sup>, Y. Wang<sup>4</sup>

<sup>1</sup>Royal Observatory of Belgium, Ringlaan 3, B-1180 Brussels, Belgium

<sup>2</sup>AWE plc, Aldermaston, Reading, RG7 4PR, United Kingdom

<sup>3</sup>Space Telescope Science Institute, 3700 San Martin Drive, Baltimore, MD 21218, USA

<sup>4</sup>Dept. of Physics & Astronomy, University of Kentucky, Lexington, KY 40506, USA

<sup>5</sup>Dept. of Physics & Astronomy and Center for Simulational Physics, University of Georgia, Athens, GA 30602, USA

Accepted. Received

## ABSTRACT

Modern spectral synthesis codes need the thermally averaged free-free Gaunt factor defined over a very wide range of parameter space in order to produce an accurate prediction for the spectrum emitted by an ionized plasma. Until now no set of data exists that would meet this need in a fully satisfactory way. We have therefore undertaken to produce a table of very accurate non-relativistic Gaunt factors over a much wider range of parameters than has ever been produced before. We first produced a table of non-averaged Gaunt factors, covering the parameter space  $^{10} \log \epsilon_i = -20$  to  $+10$  and  $^{10} \log w = -30$  to  $+25$ . We then continued to produce a table of thermally averaged Gaunt factors covering the parameter space  $^{10} \log \gamma^2 = -6$  to  $+10$  and  $^{10} \log u = -16$  to  $+13$ . Finally we produced a table of the frequency integrated Gaunt factor covering the parameter space  $^{10} \log \gamma^2 = -6$  to  $+10$ . All the data presented in this paper are available online.

**Key words:** atomic data — plasmas — radiation mechanisms: thermal — ISM: general — radio continuum: general

## 1 INTRODUCTION

One of the oldest problems in quantum mechanics is calculating the line and continuous spectrum of hydrogenic ions. An early overview of the problem can be found in Menzel & Pekeris (1935, hereafter MP35). In this paper we will revisit the problem of calculating the free-free emission and absorption of such an ion.

The problem is customarily described by using the free-free Gaunt factor (Gaunt 1930), which is a multiplicative factor describing the deviation from classical theory. For brevity we will sometimes refer to the free-free Gaunt factor simply as the Gaunt factor below. Further details on the definition of the Gaunt factor can be found in MP35 and Karzas & Latter (1961, hereafter KL61) and will not be repeated here. Several papers have been dedicated to calculating the Gaunt factor in the past (e.g., MP35; KL61; Hummer 1988; Sutherland 1998, hereafter S98) and they progressively increased the size of the parameter space and improved the precision of the results. However, despite the long history of the problem, there is still no fully satisfactory set of Gaunt

factors available. This is a result of the fact that calculating the necessary data is challenging, even with the aid of modern computers.

A modern spectral synthesis code, such as Cloudy (Ferland et al. 2013), needs accurate values for the Gaunt factor over a very wide range of parameter space. Unfortunately none of the existing data sets fulfills that requirement. Analytic expressions for the limiting behavior of the Gaunt factor have been derived in the past (for an overview see Hummer 1988 and Beckert et al. 2000). However, extrapolating tabulated data of a two-dimensional function beyond their limits using these expressions is awkward and can easily lead to discontinuities in the final result. This is exactly what has happened in the current release of Cloudy (version c13.03). This fact has prompted us to recalculate the Gaunt factor, using ab-initio theory, to a high degree of accuracy over a very wide range of parameter space. The coverage of the new tables will be large enough to avoid any need for extrapolation. These results will be included in the upcoming release of Cloudy. The paper that comes closest to what we are undertaking here is S98 and we will be following this paper closely. We will also present a comparison of our re-

\* p.vanhoof@oma.be

sults to those of S98. In the process we will fix several errors that we found in the literature.

In Sect. 2 we will describe the calculation of non-averaged free-free Gaunt factors. In Sect. 3 we will describe the calculation of the thermally averaged Gaunt factors, and in Sect. 4 we will describe the calculation of the total Gaunt factor which is integrated over frequency. Finally, in Sect. 5 we will present a summary of our results. All the data presented in this paper are available in electronic form from MNRAS as well as the Cloudy web site at <http://data.nublado.org/gauntff/>.

## 2 THE FREE-FREE GAUNT FACTOR

We will be considering the process where an unbound electron is moving through the Coulomb field of a positively charged nucleus and absorbs a photon of energy  $h\nu$  in the process. It will be assumed that the nucleus is a point-like charge, which implies that the theory is only strictly valid for fully stripped ions, though it is routinely used as an approximation for other ions as well. The theory we use is non-relativistic and is therefore not valid for very high-temperature plasmas. Comparison of the results we present below with those of Nozawa et al. (1998) shows that our results should be accurate up to electron temperatures of roughly 100 MK. For higher temperatures our results will start deviating increasingly from the correct relativistic results. We will nevertheless include results for those temperatures in our tables simply because Cloudy needs these data. Gaunt factors calculated using the relativistic Elwert approximation will be presented in a forthcoming paper.

### 2.1 Basic definitions

We follow the theory and notations given in KL61, S98, and references therein. Here we will only repeat those definitions needed to compute the free-free Gaunt factor. The formulas needed to calculate the opacity and emissivity can be found in KL61. We denote the scaled initial and final energy of the electron as

$$\epsilon_i = \frac{E_i}{Z^2 \text{Ry}} \quad \text{and} \quad \epsilon_f = \frac{E_f}{Z^2 \text{Ry}}, \quad (1)$$

where  $E$  is the energy of the electron,  $Z$  is the charge of the nucleus in elementary charge units, and Ry is the infinite-mass Rydberg unit of energy given by

$$1 \text{ Ry} = \alpha^2 m_e c^2 / 2 \approx 2.17987 \times 10^{-18} \text{ J},$$

where  $\alpha$  is the fine-structure constant,  $m_e$  is the electron mass, and  $c$  is the speed of light. We can also define the scaled photon energy as

$$w \equiv \epsilon_f - \epsilon_i = \frac{h\nu}{Z^2 \text{Ry}}. \quad (2)$$

From the scaled energies we can derive the quantities

$$\eta_i = \frac{1}{\sqrt{\epsilon_i}} \quad \text{and} \quad \eta_f = \frac{1}{\sqrt{\epsilon_f}} = \frac{1}{\sqrt{\epsilon_i + w}} \quad (3)$$

as well as

$$k_i = \frac{1}{\eta_i} \quad \text{and} \quad k_f = \frac{1}{\eta_f} \quad (4)$$

From these definitions it is clear that  $\eta_i$  and  $\eta_f$  are real numbers which are larger than zero. Furthermore, since  $w > 0$  we have  $\eta_i > \eta_f$ .

We will also use the following custom variables

$$x = -\frac{4k_i k_f}{(k_i - k_f)^2} = -\frac{4\eta_i \eta_f}{(\eta_i - \eta_f)^2}, \quad (5)$$

$$\alpha = \frac{k_i}{k_f} = \frac{\eta_f}{\eta_i}, \quad (6)$$

and

$$\beta = \frac{1 + \alpha}{1 - \alpha} = \frac{k_f + k_i}{k_f - k_i} = \frac{\eta_i + \eta_f}{\eta_i - \eta_f}. \quad (7)$$

From these definitions it is clear that  $x \in (-\infty, 0)$ ,  $\alpha \in (0, 1)$  and  $\beta \in (1, \infty)$ .

### 2.2 Exact calculation of the free-free Gaunt factor

The free-free Gaunt factor is given by Eq. 16 of KL61 (based on Biedenharn 1956)

$$g_{\text{ff}} = \frac{2\sqrt{3}}{\pi\eta_i\eta_f} \left[ (\eta_i^2 + \eta_f^2 + 2\eta_i^2\eta_f^2) I_0 - 2\eta_i\eta_f(1 + \eta_i^2)^{1/2}(1 + \eta_f^2)^{1/2} I_1 \right] I_0. \quad (8)$$

Here  $I_0$  and  $I_1$  are defined by

$$I_l = \frac{1}{4} \left[ \frac{4k_i k_f}{(k_i - k_f)^2} \right]^{l+1} e^{\pi|\eta_i - \eta_f|/2} \times \frac{|\Gamma(l+1+i\eta_i)\Gamma(l+1+i\eta_f)|}{\Gamma(2l+2)} G_l, \quad (9)$$

where  $\Gamma$  is the gamma function. In turn  $G_l$  is defined by

$$G_l = |\beta|^{-i\eta_i - i\eta_f} {}_2F_1(l+1-i\eta_f, l+1-i\eta_i; 2l+2; x), \quad (10)$$

where  ${}_2F_1(a, b; c; x)$  is the hypergeometric function. This function can be evaluated using the Taylor series expansion

$${}_2F_1(a, b; c; x) = \sum_{n=0}^{\infty} \frac{(a)_n (b)_n}{(c)_n} \frac{x^n}{n!}, \quad (11)$$

where the Pochhammer symbol  $(a)_n$  is defined as

$$(a)_n \equiv \Gamma(a+n)/\Gamma(a).$$

This series expansion has a radius of convergence  $|x| < 1$ . For values  $|x| > 1$ , the standard transformation used in the literature is given by Eq. 15.3.7 of Abramowitz & Stegun (1972):

$$\begin{aligned} {}_2F_1(a, b; c; x) = & \frac{\Gamma(c)\Gamma(b-a)}{\Gamma(b)\Gamma(c-a)} (-x)^{-a} {}_2F_1\left(a, 1-c+a; 1-b+a; \frac{1}{x}\right) \\ & + \frac{\Gamma(c)\Gamma(a-b)}{\Gamma(a)\Gamma(c-b)} (-x)^{-b} {}_2F_1\left(b, 1-c+b; 1-a+b; \frac{1}{x}\right). \end{aligned} \quad (12)$$

Using Eq. 12 assures that  $|x| \leq 1$  for all evaluations of the hypergeometric function. However, we found that for  $|x|$  close to 1, the evaluation of the Taylor series in Eq. 11 is extremely slow. We therefore decided to use an additional transformation given in Eq. 15.3.4 of Abramowitz & Stegun (1972):

$${}_2F_1(a, b; c; x) = (1-x)^{-a} {}_2F_1\left(a, c-b; c; \frac{x}{x-1}\right). \quad (13)$$

For  $-1 \leq x < 0$  we will combine Eq. 10 with Eq. 13, which yields

$$\begin{aligned} G_l &= \beta^{-i\eta_i - i\eta_f} (1-x)^{-l-1+i\eta_f} \\ &\quad \times {}_2F_1\left(l+1-i\eta_f, l+1+i\eta_i; 2l+2; \frac{x}{x-1}\right) \Rightarrow \\ G_l &= \beta^{-2l-2+i\eta_f-i\eta_i} \\ &\quad \times {}_2F_1\left(l+1+i\eta_i, l+1-i\eta_f; 2l+2; \frac{x}{x-1}\right). \quad (14) \end{aligned}$$

Here we used the fact that  $\beta$  is positive, as well as the identities

$${}_2F_1(a, b; c; x) = {}_2F_1(b, a; c; x) \quad \text{and} \quad 1-x = \beta^2.$$

For  $x < -1$  we will combine Eq. 10 with Eqs. 12 and 13, (in that order, this is equivalent to using Eq. 15.3.8 in Abramowitz & Stegun 1972), which yields:

$$\begin{aligned} G_l &= \left[ \frac{\Gamma(2l+2)\Gamma(i\eta_f - i\eta_i)}{\Gamma(l+1-i\eta_i)\Gamma(l+1+i\eta_f)} \beta^{-2l-2+i\eta_f-i\eta_i} \right. \\ &\quad \times {}_2F_1\left(l+1+i\eta_i, l+1-i\eta_f; 1+i\eta_i - i\eta_f; \frac{1}{1-x}\right) \\ &\quad \left. + \frac{\Gamma(2l+2)\Gamma(i\eta_i - i\eta_f)}{\Gamma(l+1+i\eta_i)\Gamma(l+1-i\eta_f)} \beta^{-2l-2+i\eta_i-i\eta_f} \right. \\ &\quad \left. \times {}_2F_1\left(l+1-i\eta_i, l+1+i\eta_f; 1-i\eta_i + i\eta_f; \frac{1}{1-x}\right) \right] \Rightarrow \\ G_l &= 2\Re \left[ \frac{\Gamma(2l+2)\Gamma(i\eta_f - i\eta_i)}{\Gamma(l+1-i\eta_i)\Gamma(l+1+i\eta_f)} \beta^{-2l-2+i\eta_f-i\eta_i} \right. \\ &\quad \left. \times {}_2F_1\left(l+1+i\eta_i, l+1-i\eta_f; 1+i\eta_i - i\eta_f; \frac{1}{1-x}\right) \right], \quad (15) \end{aligned}$$

where we additionally used the identities

$${}_2F_1(\bar{a}, \bar{b}; \bar{c}; \bar{z}) = \overline{{}_2F_1(a, b; c; z)} \quad \text{and} \quad \Gamma(\bar{z}) = \overline{\Gamma(z)}.$$

Using these transformations instead of the standard ones found in the literature has a number of advantages.

(i) For all values of  $x$  only a single evaluation of the hypergeometric function is needed for each evaluation of  $G_l$ .

(ii) The last argument of the hypergeometric function is between 0 and  $1/2$  for all values of  $x$ . This greatly speeds up the evaluation of this function.

(iii) For each evaluation of  $g_{\text{ff}}$  only 2 or 3 evaluations of the gamma function are needed by using  $\Gamma(\bar{z}) = \overline{\Gamma(z)}$  and  $\Gamma(z+1) = z\Gamma(z)$ , implying that we can reuse the results for  $I_0$  when calculating  $I_1$ . This discounts the trivial evaluation of  $\Gamma(2l+2)$  which is hardwired in the code.

Numerically evaluating Eq. 8 can lead to severe cancellation problems. For this reason we decided to implement our code in C++ using arbitrary precision floating point variables. We use libgmp version 5.1.2 for the basic arithmetic functions, libmpfr 3.1.2 for the transcendental functions, and libmpfr++ by Pavel Holoborodko (version Nov. 2010) to get a convenient C++ wrapper around libgmp and libmpfr. These libraries allow the user to choose the number of bits  $b$  of the mantissa of the floating point number as a free parameter. In our implementation we start our calculations

using  $b = 128$ . We then calculate the Gaunt factor including an estimate of its relative error (taking into account cancellation effects in intermediate results). If the relative error is less than  $10^{-15}$  the result is accepted, otherwise  $b$  will be doubled and the calculation is started again. This procedure is repeated until either the Gaunt factor is accepted or  $b$  exceeds a maximum precision of the mantissa. For most calculations we use  $b_{\text{max}} = 4096$ , but in some cases we allowed it to go higher. The precision of the floating point numbers that we use is approximately  $b/2 \log_{10}$  decimal places. So this ranges between  $\sim 38$  decimal places for  $b = 128$  and  $\sim 1233$  decimal places for  $b = 4096$ . The choice of  $b$  is illustrated in Table 1 where we give the value of  ${}^2\log b$  used as a function of  $\epsilon_i$  and  $w$  in the region where the cancellation problems are worst.

In libmpfr there is no routine to calculate the complex gamma function. So we implemented an arbitrary precision routine ourselves based on Spouge's approximation (Spouge 1994). This algorithm also suffers from severe cancellation problems, so internal calculations are done using twice the number of bits used for the Gaunt factor itself.

In some parts of the parameter space even using a 4096 bit mantissa is not enough to successfully calculate the Gaunt factor due to complete loss of precision in intermediate results. In that case, we will use the series expansion presented in Sect. 2.3 since doubling the number of bits in the mantissa further would lead to unacceptable CPU time consumption. The area where this can happen has a roughly triangular shape inside the following boundaries

$$w \leq 10^{-6} \quad (16)$$

and

$$\epsilon_i^{3/2}/w \leq 10^{-4}. \quad (17)$$

Note that we attempt an exact calculation first, even inside this region, and only if that fails will we use the series expansion discussed below.

To speed up the calculations, all tables were calculated using a parallel version of the code using the message passing interface (MPI).

### 2.3 Approximating the free-free Gaunt factor

In the region where the exact calculation of the Gaunt factor fails, we will use the series expansion given in MP35. When testing this procedure we noted that the highest order term of Eq (1.41) of MP35 is incorrect. We therefore repeated the derivation outlined in the Appendix of MP35 to fix the error, and added an extra term in the process. The details can be found in Appendix A. The resulting corrected formula is (note that in MP35,  $\kappa \equiv \eta_f$  and  $l \equiv \eta_i$ )

$$\begin{aligned} g_{\text{ff}} &= 1 + c_1 \frac{(1 + \eta_f^2/\eta_i^2)}{(1 - \eta_f^2/\eta_i^2)^{2/3} \eta_f^{2/3}} - c_2 \frac{(1 - {}^{4/3}\eta_f^2/\eta_i^2 + \eta_f^4/\eta_i^4)}{(1 - \eta_f^2/\eta_i^2)^{4/3} \eta_f^{4/3}} \\ &\quad - c_3 \frac{(1 - {}^{1/3}\eta_f^2/\eta_i^2 - {}^{1/3}\eta_f^4/\eta_i^4 + \eta_f^6/\eta_i^6)}{(1 - \eta_f^2/\eta_i^2)^{6/3} \eta_f^{6/3}} + R, \quad (18) \end{aligned}$$

with  $(1 - \eta_f^2/\eta_i^2) \eta_f \gg 1$  and

$$c_1 = \frac{\Gamma(1/3)}{5 \cdot 12^{1/3} \Gamma(2/3)} = 0.1728260369\dots,$$

$$c_2 = \frac{18 \Gamma(2/3)}{35 \cdot 12^{2/3} \Gamma(1/3)} = 0.04959570168\dots,$$

$$c_3 = \frac{3}{175} = 0.01714285714\dots,$$

and

$$\frac{0.00135}{(1 - \eta_f^2/\eta_i^2)^{8/3} \eta_f^{8/3}} < R < \frac{0.025}{(1 - \eta_f^2/\eta_i^2)^{8/3} \eta_f^{8/3}}. \quad (19)$$

Eq. 19 was derived by comparing the series expansion with exact calculations for various values of the ratio  $\eta_f/\eta_i$  between 0 and 1. This is possible because the numerator of  $R$  is a polynomial in  $\eta_f/\eta_i$ , and for every value of the ratio  $\eta_f/\eta_i$  a combination of values  $\eta_f$  and  $\eta_i$  can be found for which the exact calculation succeeds. Thus the minimum and maximum value of the numerator of  $R$  can be determined. We will use the upper limit of Eq. 19 as an estimate for the error in the series expansion in our calculations. The exact calculation of the Gaunt factor may fail in the triangular region bounded by Eqs. 16 and 17. Using Eq. 19 we could determine that the absolute error in Eq. 18 is certainly less than  $5.5 \times 10^{-10}$  everywhere in this region. The worst case behavior of Eq. 18 is at the corner of the triangular area delimiting its use (i.e.,  $^{10}\log \epsilon_i = -6^{2/3}$ ,  $^{10}\log w = -6$ ). We explore the error in the series expansion further in Table 1 where we show the residual of the series expansion as a function of  $\epsilon_i$  and  $w$  in this region. It is clear that the residual is less than  $10^{-10}$  everywhere, which is more than sufficient for our needs.

We can understand this result also in a different manner. Near the boundary given by Eq. 17, the criterion  $w/\epsilon_i^{3/2} \geq 10^4$  can be rewritten as follows:

$$\begin{aligned} w/\epsilon_i^{3/2} &= (\epsilon_f - \epsilon_i)/\epsilon_i^{3/2} \approx (\epsilon_f - \epsilon_i)/\epsilon_f^{3/2} = (1 - \epsilon_i/\epsilon_f)/\epsilon_f^{1/2} \\ &= (1 - \eta_f^2/\eta_i^2) \eta_f \gtrsim 10^4. \end{aligned}$$

This clearly shows that the remainder  $R$  in Eq. 18 is guaranteed to be very small. The combination of this criterion with Eq. 16 also guarantees that  $\eta_i \gg 1$  and  $\eta_f \gg 1$ , which are also necessary conditions for the series expansion to be valid.

## 2.4 A table of Gaunt factors

Using the procedure outlined in the previous sections we computed a large grid of Gaunt factors, covering the range  $^{10}\log \epsilon_i = -20(0.2)10$  and  $^{10}\log w = -30(0.2)25$ . The notation  $-20(0.2)10$  indicates that the Gaunt factor was tabulated for all values of  $^{10}\log \epsilon_i$  ranging from  $-20$  to  $10$  in increments of  $0.2$  dex, and similarly for  $^{10}\log w$ . This range vastly extends the parameter range computed by S98. The data are shown in Fig. 1. The full table is available in electronic form (see Sect. 5). The electronic table gives the Gaunt factors in 11 significant digits and is accurate in all digits, apart from possible rounding errors in some entries computed with the series expansion. In addition to the table, we also provide simple programs which allow the user to interpolate the table. Testing of the interpolation algorithm showed that the relative error was less than  $1.5 \times 10^{-4}$  everywhere.

In Table 2 we give an excerpt from the electronic table covering the same parameter space presented in S98. Apart

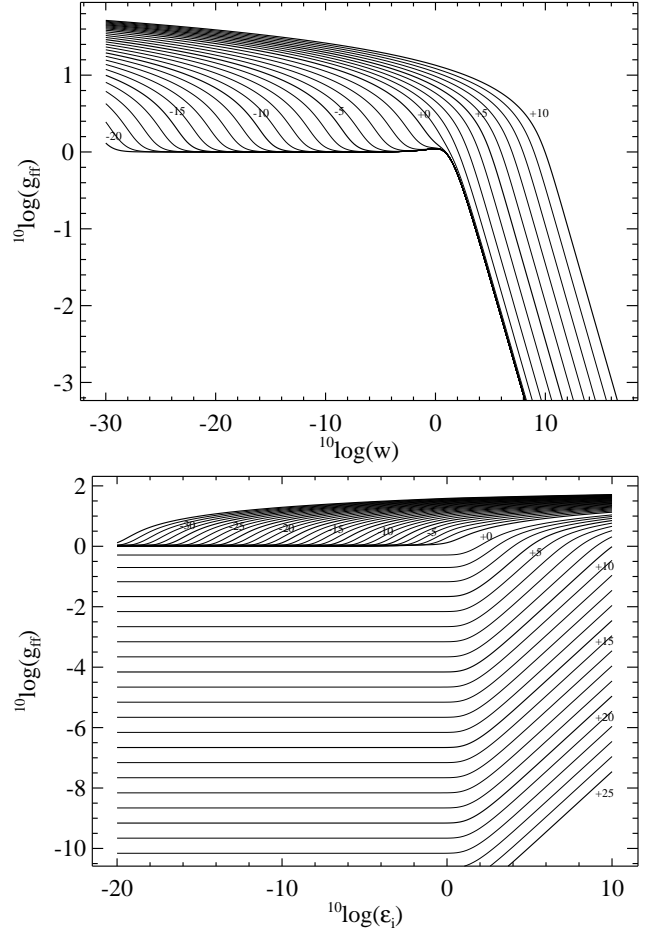


**Figure 1.** The base-10 logarithm of the free-free Gaunt factor as a function of  $w$  (top panel) and  $\epsilon_i$  (bottom panel). Thick curves are labeled with the values of  $^{10}\log \epsilon_i$  (top panel) and  $^{10}\log w$  (bottom panel) in increments of 5 dex. The thin curves have a spacing of 1 dex.

from the obvious fact that in S98 the parameters  $\epsilon_i$  and  $w$  were transposed, both in their Table 1 and Fig. 1 (but not the electronic version of this table), we can also see that the data in S98 don't reach the claimed precision everywhere. Comparing the electronic version of the table from S98 with our calculations (which covers a slightly larger range in parameter space than Table 1 in S98) we find that the largest discrepancy is almost 7.3% for the entry for  $^{10}\log \epsilon_i = -9$  and  $^{10}\log w = -8$ . Also the entries near the edge towards the upper right corner of Table 1 in S98 don't reach the claimed precision. One example is the entry for  $^{10}\log \epsilon_i = -2^{2/3}$  and  $^{10}\log w = -8$  in the electronic table with a discrepancy of slightly more than 0.57%. The median relative discrepancy is better than  $10^{-8}$  however, indicating that the majority of the entries in the electronic table of S98 are accurate in all printed digits.

The claim in S98 that the Gaunt factors tend to a limiting value for  $\epsilon_i \rightarrow 0$  is correct, but the numeric values for this limit given in his Table 1 are not accurate for low values of  $w$ . From Eq. 18 we can derive the following series expansion for this limit

$$g_{\text{ff}}(0, w) = 1 + c_1 w^{1/3} - c_2 w^{2/3} - c_3 w + O(w^{4/3}), \quad (20)$$

**Table 1.** The residual  $R$  of the series expansion for  $g_{\text{ff}}$  given in Eq. 18. Entries 1.29–12 mean  $1.29 \times 10^{-12}$  and entries marked with dots are outside the region of validity of the series expansion. The number between parentheses is  $^2 \log b$ , the number of bits of the mantissa used in the calculation of the exact Gaunt factor.

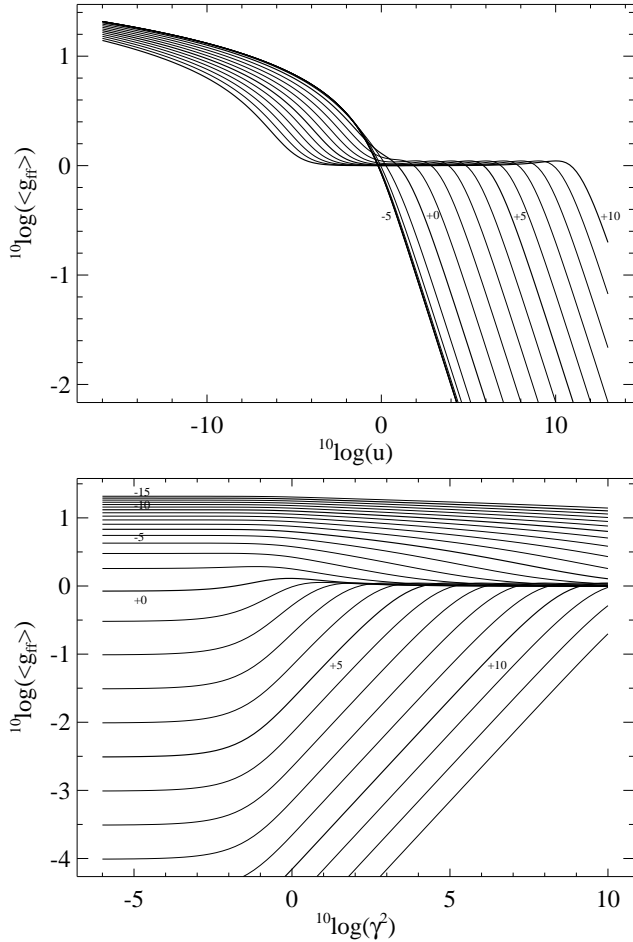
$^{10} \log w$	–8.50	–8.25	–8.00	$^{10} \log \epsilon_i$		–7.25	–7.00	–6.75
				–7.75	–7.50			
–8.75	1.29–12 (11)	...	...	...	...	...	...	...
–8.50	4.52–13 (11)	...	...	...	...	...	...	...
–8.25	1.92–13 (12)	9.73–13 (11)	...	...	...	...	...	...
–8.00	1.16–13 (12)	4.15–13 (11)	2.10–12 (11)	...	...	...	...	...
–7.75	1.22–13 (12)	2.49–13 (12)	8.93–13 (11)	...	...	...	...	...
–7.50	2.08–13 (12)	2.63–13 (12)	5.37–13 (11)	1.92–12 (11)	...	...	...	...
–7.25	4.27–13 (12)	4.47–13 (12)	5.67–13 (11)	1.16–12 (11)	4.14–12 (10)	...	...	...
–7.00	9.20–13 (12)	9.18–13 (12)	9.61–13 (11)	1.22–12 (11)	2.49–12 (10)	...	...	...
–6.75	2.00–12 (13)	1.98–12 (12)	1.98–12 (11)	2.07–12 (11)	2.62–12 (11)	5.36–12 (10)	...	...
–6.50	4.32–12 (13)	4.29–12 (12)	4.26–12 (11)	4.25–12 (11)	4.45–12 (11)	5.64–12 (10)	1.15–11 (10)	...
–6.25	9.34–12 (12)	9.30–12 (12)	9.23–12 (12)	9.15–12 (11)	9.14–12 (11)	9.57–12 (10)	1.21–11 (10)	...
–6.00	2.01–11 (12)	2.01–11 (12)	2.00–11 (12)	1.98–11 (12)	1.97–11 (10)	1.96–11 (10)	2.06–11 (10)	2.61–11 (9)

**Table 2.**  $g_{\text{ff}}(\epsilon_i, w)$ . Entries 1.0011+0 mean  $1.0011 \times 10^{+0}$ . All entries in this table were calculated using the exact method. The online electronic version of this table samples a much larger parameter space, has a finer spacing, and gives more significant digits.

$^{10} \log w$	$^{10} \log \epsilon_i$								
	–8.00	–7.00	–6.00	–5.00	–4.00	–3.00	–2.00	–1.00	0.00
–8.00	1.0011+0	1.0078+0	1.0731+0	1.5690+0	3.0305+0	4.8916+0	6.7931+0	8.6931+0	1.0550+1
–7.00	1.0010+0	1.0024+0	1.0168+0	1.1527+0	1.9606+0	3.6375+0	5.5244+0	7.4236+0	9.2803+0
–6.00	1.0018+0	1.0021+0	1.0052+0	1.0359+0	1.3062+0	2.4606+0	4.2607+0	6.1544+0	8.0108+0
–5.00	1.0037+0	1.0038+0	1.0044+0	1.0111+0	1.0763+0	1.5709+0	3.0304+0	4.8871+0	6.7414+0
–4.00	1.0079+0	1.0079+0	1.0081+0	1.0095+0	1.0238+0	1.1589+0	1.9627+0	3.6332+0	5.4727+0
–3.00	1.0168+0	1.0168+0	1.0168+0	1.0171+0	1.0202+0	1.0506+0	1.3172+0	2.4589+0	4.2093+0
–2.00	1.0348+0	1.0348+0	1.0348+0	1.0348+0	1.0355+0	1.0420+0	1.1053+0	1.5837+0	2.9811+0
–1.00	1.0679+0	1.0679+0	1.0679+0	1.0679+0	1.0680+0	1.0693+0	1.0826+0	1.2067+0	1.9284+0
0.00	1.1040+0	1.1040+0	1.1040+0	1.1040+0	1.1040+0	1.1042+0	1.1065+0	1.1290+0	1.3149+0
1.00	9.5465–1	9.5465–1	9.5465–1	9.5465–1	9.5465–1	9.5466–1	9.5479–1	9.5610–1	9.7004–1
2.00	5.1462–1	5.1462–1	5.1462–1	5.1462–1	5.1462–1	5.1462–1	5.1462–1	5.1461–1	5.1543–1
3.00	1.9870–1	1.9870–1	1.9870–1	1.9870–1	1.9870–1	1.9870–1	1.9870–1	1.9870–1	1.9905–1
4.00	6.7151–2	6.7151–2	6.7151–2	6.7151–2	6.7151–2	6.7151–2	6.7151–2	6.7151–2	6.7275–2
5.00	2.1693–2	2.1693–2	2.1693–2	2.1693–2	2.1693–2	2.1693–2	2.1693–2	2.1693–2	2.1733–2
6.00	6.9065–3	6.9065–3	6.9065–3	6.9065–3	6.9065–3	6.9065–3	6.9065–3	6.9065–3	6.9194–3
7.00	2.1887–3	2.1887–3	2.1887–3	2.1887–3	2.1887–3	2.1887–3	2.1887–3	2.1887–3	2.1928–3
8.00	6.9260–4	6.9260–4	6.9260–4	6.9260–4	6.9260–4	6.9260–4	6.9260–4	6.9260–4	6.9390–4
9.00	2.1907–4	2.1907–4	2.1907–4	2.1907–4	2.1907–4	2.1907–4	2.1907–4	2.1907–4	2.1948–4

$^{10} \log w$	$^{10} \log \epsilon_i$								
	1.00	2.00	3.00	4.00	5.00	6.00	7.00	8.00	9.00
–8.00	1.2129+1	1.3453+1	1.4728+1	1.5998+1	1.7268+1	1.8537+1	1.9807+1	2.1076+1	2.2345+1
–7.00	1.0859+1	1.2183+1	1.3458+1	1.4729+1	1.5998+1	1.7268+1	1.8537+1	1.9807+1	2.1076+1
–6.00	9.5896+0	1.0914+1	1.2189+1	1.3459+1	1.4729+1	1.5998+1	1.7268+1	1.8537+1	1.9807+1
–5.00	8.3201+0	9.6441+0	1.0919+1	1.2190+1	1.3459+1	1.4729+1	1.5998+1	1.7268+1	1.8537+1
–4.00	7.0507+0	8.3746+0	9.6500+0	1.0920+1	1.2190+1	1.3459+1	1.4729+1	1.5998+1	1.7268+1
–3.00	5.7815+0	7.1052+0	8.3805+0	9.6506+0	1.0920+1	1.2190+1	1.3459+1	1.4729+1	1.5998+1
–2.00	4.5142+0	5.8358+0	7.1111+0	8.3811+0	9.6507+0	1.0920+1	1.2190+1	1.3459+1	1.4729+1
–1.00	3.2610+0	4.5672+0	5.8416+0	7.1117+0	8.3812+0	9.6507+0	1.0920+1	1.2190+1	1.3459+1
0.00	2.0912+0	3.3046+0	4.5726+0	5.8422+0	7.1117+0	8.3812+0	9.6507+0	1.0920+1	1.2190+1
1.00	1.1971+0	2.0838+0	3.3070+0	4.5730+0	5.8423+0	7.1117+0	8.3812+0	9.6507+0	1.0920+1
2.00	5.9451–1	1.0564+0	2.0692+0	3.3065+0	4.5730+0	5.8423+0	7.1117+0	8.3812+0	9.6507+0
3.00	2.3001–1	4.2101–1	9.9968–1	2.0633+0	3.3062+0	4.5730+0	5.8423+0	7.1117+0	8.3812+0
4.00	7.7810–2	1.4373–1	3.6723–1	9.8075–1	2.0613+0	3.3061+0	4.5730+0	5.8423+0	7.1117+0
5.00	2.5139–2	4.6492–2	1.2019–1	3.5069–1	9.7468–1	2.0607+0	3.3060+0	4.5730+0	5.8423+0
6.00	8.0040–3	1.4804–2	3.8321–2	1.1322–1	3.4551–1	9.7275–1	2.0605+0	3.3060+0	4.5730+0
7.00	2.5365–3	4.6917–3	1.2146–2	3.5934–2	1.1107–1	3.4388–1	9.7214–1	2.0604+0	3.3060+0
8.00	8.0266–4	1.4846–3	3.8436–3	1.1373–2	3.5200–2	1.1039–1	3.4336–1	9.7194–1	2.0604+0
9.00	2.5388–4	4.6959–4	1.2157–3	3.5972–3	1.1135–2	3.4969–2	1.1018–1	3.4320–1	9.7188–1



**Figure 2.** The base-10 logarithm of the thermally averaged free-free Gaunt factor as a function of  $u$  (top panel) and  $\gamma^2$  (bottom panel). Thick curves are labeled with the values of  $^{10}\log\gamma^2$  (top panel) and  $^{10}\log u$  (bottom panel) in increments of 5 dex. The thin curves have a spacing of 1 dex. In the top panel the Gaunt factors approach a limiting curve for  $^{10}\log\gamma^2 < -2$  and are indistinguishable in the plot.

for  $w \ll 1$ . Here we used the fact that  $\eta_f/\eta_i = 0$  and  $\eta_f = w^{-1/2}$  for  $\epsilon_i = 0$ . In Hummer (1988) additional terms can be found for this series expansion in his Eq. 2.23a.

### 3 THE THERMALLY AVERAGED FREE-FREE GAUNT FACTOR

When modeling astrophysical plasmas, it is commonly assumed that the electrons have a Maxwellian energy distribution, characterized by the electron temperature  $T_e$ . We therefore need to average the Gaunt factors derived in Sect. 2 over such a distribution. For this we define the following scaled quantities

$$\gamma^2 = \frac{Z^2 \text{Ry}}{kT_e} \quad \text{and} \quad u = \frac{h\nu}{kT_e}. \quad (21)$$

Using these definitions, we can give the following expression for the thermally averaged Gaunt factor

$$\langle g_{\text{ff}}(\gamma^2, u) \rangle = \int_0^\infty e^{-x} g_{\text{ff}} \left( \epsilon_i = \frac{x}{\gamma^2}, w = \frac{u}{\gamma^2} \right) dx. \quad (22)$$

For further details see KL61, S98 and references therein. Note that Eq. 14 of S98 contains a typo which has been corrected here.

Cloudy can model plasmas over a very wide parameter range:  $3 \leq T_e \leq 10^{10}$  K and  $10^{-8} \leq h\nu \leq 7.354 \times 10^6$  Ry (100 MeV), with  $Z \leq 30$ . Substituting these values into Eq. 21 yields  $-4.81 < ^{10}\log\gamma^2 < 7.68$  and  $-12.81 < ^{10}\log u < 11.59$ . This clearly shows that the parameter range for the thermally averaged Gaunt factor presented in S98 is insufficient for our needs (especially the coverage in  $u$ ). This can also be stated in a different manner. When modeling a photoionized hydrogen plasma at the canonical temperature  $T_e = 10000$  K, the longest wavelength that can be modeled with the S98 data is  $\sim 1.44$  cm. Radio observations at longer wavelengths are routinely made and Cloudy should be able to model those. In the view of the stated facts, we have used a much larger parameter space in our calculations:  $^{10}\log\gamma^2 = -6(0.2)10$  and  $^{10}\log u = -16(0.2)13$ . This is larger even than the current needs of Cloudy and anticipates possible future modifications to the code, such as the addition of higher- $Z$  elements and/or lowering the low-frequency cut-off.

The integration shown in Eq. 22 is carried out using an adaptive stepsize algorithm based on Eq. 4.1.20 of Press et al. (1992) for carrying out a single step. This algorithm is open at the lefthand side, thus avoiding the awkward evaluation of the integrand at  $x = 0$ . During the evaluation of the integral, at every step an estimate is made of the remainder of the integral to infinity by assuming that  $g_{\text{ff}}$  is constant. This estimate is reasonable as  $g_{\text{ff}}$  is only slowly increasing. The integration is terminated when this estimate is less than 1% of the requested tolerance. The requested tolerance of the thermally averaged Gaunt factor is a free parameter and the routine calculates an estimate of the actual error in the final result taking into account both the imprecisions due to the finite stepsize and the error in the non-averaged Gaunt factor. For the electronic table we used a requested relative tolerance of  $10^{-5}$ . The data are presented in Fig. 2 and Table 3. The data can also be downloaded in electronic form (see Sect. 5). Note that the data shown in Table 3 were calculated to a higher precision to assure that all numbers shown are correctly rounded. In addition to the electronic table, we also provide simple programs which allow the user to interpolate the table. Testing of the interpolation algorithm showed that the relative error was less than  $1.5 \times 10^{-4}$  everywhere.

Comparing our results with those of S98, we noted the serious problem that the parameters  $^{10}\log\gamma^2$  and  $^{10}\log u$  were transposed in Table 2 of S98, as well as in the electronic version of that table. After correcting for this error, there were some minor discrepancies when we compared the numerical values in the electronic table of S98 to our results. The largest relative error is for  $^{10}\log\gamma^2 = -1.8$  and  $^{10}\log u = 0.5$  and amounts to almost 0.13%. The median relative discrepancy is approximately  $5 \times 10^{-5}$ . So it appears that the discrepancies we reported in Sect. 2.4 did not have a significant impact on the calculation of the thermally averaged Gaunt factor by S98.

**Table 3.**  $\langle g_{\text{ff}}(\gamma^2, u) \rangle$ . Entries 1.0601+1 mean  $1.0601 \times 10^{+1}$ . All entries have an approximate relative error of  $3 \times 10^{-8}$ , assuring that they are all correctly rounded as shown. The online electronic version of this table samples a much larger parameter space, has a finer spacing, and is calculated using an approximate relative tolerance of  $10^{-5}$  (an estimate for the error in each number is included in the table).

$^{10} \log u$	$^{10} \log \gamma^2$								
	-4.00	-3.00	-2.00	-1.00	0.00	1.00	2.00	3.00	4.00
-8.00	1.0601+1	1.0598+1	1.0573+1	1.0449+1	1.0073+1	9.4852+0	8.8548+0	8.2207+0	7.5863+0
-7.00	9.3319+0	9.3280+0	9.3033+0	9.1795+0	8.8036+0	8.2160+0	7.5859+0	6.9524+0	6.3194+0
-6.00	8.0624+0	8.0586+0	8.0340+0	7.9103+0	7.5347+0	6.9477+0	6.3190+0	5.6882+0	5.0606+0
-5.00	6.7931+0	6.7894+0	6.7651+0	6.6421+0	6.2678+0	5.6835+0	5.0601+0	4.4399+0	3.8322+0
-4.00	5.5243+0	5.5213+0	5.4983+0	5.3780+0	5.0091+0	4.4354+0	3.8318+0	3.2474+0	2.7008+0
-3.00	4.2581+0	4.2577+0	4.2402+0	4.1307+0	3.7818+0	3.2438+0	2.7011+0	2.2128+0	1.8041+0
-2.00	3.0049+0	3.0125+0	3.0153+0	2.9436+0	2.6563+0	2.2134+0	1.8072+0	1.4932+0	1.2769+0
-1.00	1.8154+0	1.8368+0	1.8882+0	1.9244+0	1.7826+0	1.5086+0	1.2884+0	1.1506+0	1.0743+0
0.00	8.5319-1	8.8158-1	9.6976-1	1.1697+0	1.2937+0	1.1987+0	1.1033+0	1.0502+0	1.0237+0
1.00	3.1011-1	3.2829-1	3.8999-1	5.8929-1	9.7260-1	1.1285+0	1.0825+0	1.0420+0	1.0202+0
2.00	1.0069-1	1.0796-1	1.3352-1	2.2811-1	5.1717-1	9.5609-1	1.1065+0	1.0693+0	1.0355+0
3.00	3.1978-2	3.4445-2	4.3211-2	7.7180-2	1.9973-1	5.1461-1	9.5479-1	1.1042+0	1.0680+0
4.00	1.0121-2	1.0918-2	1.3760-2	2.4936-2	6.7503-2	1.9870-1	5.1462-1	9.5466-1	1.1040+0
5.00	3.2014-3	3.4550-3	4.3608-3	7.9393-3	2.1807-2	6.7151-2	1.9870-1	5.1462-1	9.5465-1
6.00	1.0124-3	1.0928-3	1.3799-3	2.5160-3	6.9428-3	2.1693-2	6.7151-2	1.9870-1	5.1462-1
7.00	3.2017-4	3.4560-4	4.3647-4	7.9618-4	2.2002-3	6.9065-3	2.1693-2	6.7151-2	1.9870-1
8.00	1.0125-4	1.0929-4	1.3803-4	2.5183-4	6.9624-4	2.1887-3	6.9065-3	2.1693-2	6.7151-2

**Table 4.** The total free-free Gaunt factor as a function of  $\gamma^2$ . The relative error in the numbers is approximately  $10^{-5}$ . An online electronic version of this table is available.

$^{10} \log \gamma^2$	$\langle g_{\text{ff}}(\gamma^2) \rangle$	$^{10} \log \gamma^2$	$\langle g_{\text{ff}}(\gamma^2) \rangle$	$^{10} \log \gamma^2$	$\langle g_{\text{ff}}(\gamma^2) \rangle$	$^{10} \log \gamma^2$	$\langle g_{\text{ff}}(\gamma^2) \rangle$
-6.00	1.10382	-2.00	1.21688	2.00	1.16455	6.00	1.01003
-5.80	1.10413	-1.80	1.24243	2.20	1.14499	6.20	1.00865
-5.60	1.10453	-1.60	1.27164	2.40	1.12746	6.40	1.00745
-5.40	1.10500	-1.40	1.30383	2.60	1.11182	6.60	1.00642
-5.20	1.10562	-1.20	1.33762	2.80	1.09793	6.80	1.00553
-5.00	1.10639	-1.00	1.37085	3.00	1.08561	7.00	1.00475
-4.80	1.10737	-0.80	1.40071	3.20	1.07473	7.20	1.00409
-4.60	1.10860	-0.60	1.42404	3.40	1.06515	7.40	1.00352
-4.40	1.11015	-0.40	1.43805	3.60	1.05672	7.60	1.00302
-4.20	1.11210	-0.20	1.44095	3.80	1.04932	7.80	1.00260
-4.00	1.11457	0.00	1.43253	4.00	1.04285	8.00	1.00223
-3.80	1.11767	0.20	1.41421	4.20	1.03719	8.20	1.00191
-3.60	1.12158	0.40	1.38857	4.40	1.03224	8.40	1.00164
-3.40	1.12650	0.60	1.35859	4.60	1.02793	8.60	1.00141
-3.20	1.13269	0.80	1.32685	4.80	1.02417	8.80	1.00121
-3.00	1.14045	1.00	1.29524	5.00	1.02091	9.00	1.00104
-2.80	1.15014	1.20	1.26492	5.20	1.01807	9.20	1.00089
-2.60	1.16219	1.40	1.23649	5.40	1.01562	9.40	1.00076
-2.40	1.17704	1.60	1.21025	5.60	1.01348	9.60	1.00064
-2.20	1.19515	1.80	1.18628	5.80	1.01163	9.80	1.00055
-2.00	1.21688	2.00	1.16455	6.00	1.01003	10.00	1.00047

#### 4 THE TOTAL FREE-FREE GAUNT FACTOR

For completeness we will also include a calculation of the total free-free Gaunt factor which is integrated over frequency. This quantity is useful if one wants to calculate the total cooling due to Bremsstrahlung without spectrally resolving the process. The formula for this quantity is given by KL61 and S98

$$\langle g_{\text{ff}}(\gamma^2) \rangle = \int_0^\infty e^{-u} \langle g_{\text{ff}}(\gamma^2, u) \rangle du. \quad (23)$$

Due to the similarity of the integrals in Eqs. 22 and 23 we can use the same adaptive stepsize algorithm discussed in Sect. 3 to calculate the data. For the evaluations of  $\langle g_{\text{ff}}(\gamma^2, u) \rangle$  we used a relative tolerance of  $10^{-6}$  to prevent them dominating the error in  $\langle g_{\text{ff}}(\gamma^2) \rangle$ . The results are shown in Table 4 and Fig. 3. The computed values are also available in electronic form (see Sect. 5). The data in Table 4 show a small systematic offset w.r.t. the data in Table 3 of S98, ranging between +0.00069 for  $^{10} \log \gamma^2 = -4$  and +0.00021 for  $^{10} \log \gamma^2 = 4$ . This offset is likely due to the missing part of the integral below  $u = 10^{-4}$  in S98. The

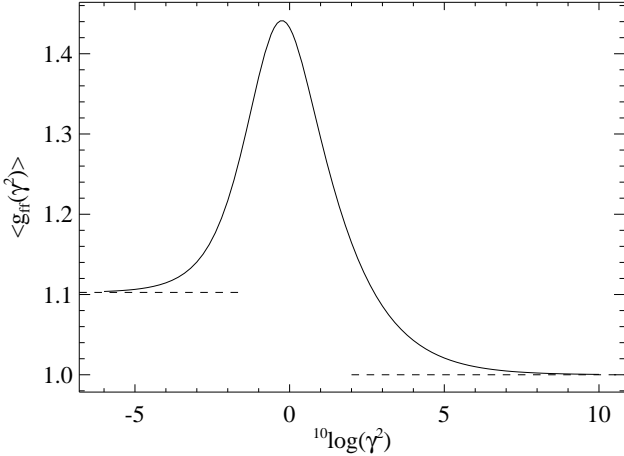


**Figure 3.** The total free-free Gaunt factor as a function of  $\gamma^2$ . The dashed lines indicate the asymptotic limits for the function.

**Table 5.** Coefficients for the rational functions defined in Eq. 26 ( $g = {}^{10}\log \gamma^2$ ). Entries 1.43... + 0 stand for  $1.43... \times 10^{+0}$ .

$-6 \leq g \leq 0.8$			
$a_0$	1.43251926625281+0	$b_0$	1.00000000000000+0
$a_1$	3.50626935257777-1	$b_1$	2.92525161994346-1
$a_2$	4.36183448595035-1	$b_2$	4.05566949766954-1
$a_3$	6.03536387105599-2	$b_3$	5.62573012783879-2
$a_4$	3.66626405363100-2	$b_4$	3.33019373823972-2
$0.8 \leq g \leq 10$			
$a_0$	1.45481634667278+0	$b_0$	1.00000000000000+0
$a_1$	-9.55399384620923-2	$b_1$	3.31149751183539-2
$a_2$	1.46327814151538-1	$b_2$	1.31127367293310-1
$a_3$	-1.41489406498468-2	$b_3$	-1.32658217746618-2
$a_4$	2.76891413242655-3	$b_4$	2.74809263365693-3

extended range in  $\gamma^2$  of the data presented here makes the limiting behavior of the function clear. Both for  $\gamma^2 \rightarrow 0$  and  $\gamma^2 \rightarrow \infty$  the function approaches an asymptotic value. Using our data we determined the following fits to the limiting behavior of the function.

$$\langle g_{\text{ff}}(\gamma^2) \rangle \approx 1.102635 + 1.186\gamma + 0.86\gamma^2 \quad \text{for } \gamma^2 < 10^{-6}, \quad (24)$$

and

$$\langle g_{\text{ff}}(\gamma^2) \rangle \approx 1 + \gamma^{-2/3} \quad \text{for } \gamma^2 > 10^{10}. \quad (25)$$

These extrapolations are expected to reach a relative precision of  $10^{-5}$  or better everywhere they are defined. The data in Table 4 can be interpolated using rational functions

$$\langle g_{\text{ff}}(g) \rangle \approx \frac{a_0 + a_1g + a_2g^2 + a_3g^3 + a_4g^4}{b_0 + b_1g + b_2g^2 + b_3g^3 + b_4g^4}, \quad (26)$$

where  $g = {}^{10}\log \gamma^2$ . To limit the degree of the rational function, we made two separate fits for the range  $-6 \leq g \leq 0.8$  and  $0.8 \leq g \leq 10$ . These fits achieve a relative error less than  $3.5 \times 10^{-5}$  everywhere in its range for the first fit and  $8.8 \times 10^{-5}$  for the second. The coefficients are given in Table 5. We have implemented Eqs. 24, 25, and 26 in simple programs which have been made available on the Cloudy web site (see Sect. 5).

## 5 SUMMARY

Modern spectral synthesis codes like Cloudy need the thermally averaged free-free Gaunt factor defined over a very wide range of parameter space in order to produce an accurate prediction for the spectrum emitted by an ionized plasma. Several authors have undertaken to calculate these atomic data in the past, however none could produce a fully satisfactory set of results that would match the needs of a code like Cloudy.

We have therefore undertaken to produce a table of very accurate non-relativistic Gaunt factors over a much wider range of parameter than has ever been produced before. For this purpose we have created a C++ program using arbitrary precision variables to avoid the severe cancellation problems that occur in the calculations, which would lead to complete loss of precision otherwise. While creating the program, we discovered several errors in the literature which have been corrected here. The most important is an error in the series expansion of the Gaunt factor reported by MP35. We also added an extra term to this series expansion to make it more accurate. We furthermore presented new transformations of the hypergeometric function, which help in speeding up the calculations. Despite all these efforts, there is still a region of parameter space where we cannot calculate the Gaunt factor to arbitrary precision because it would consume too much CPU time. In this region we fall back to the series expansion, which we show can produce sufficiently accurate results everywhere it is needed.

Using this code, we first produced a table of non-averaged Gaunt factors, covering the parameter space  ${}^{10}\log \epsilon_i = -20(0.2)10$  and  ${}^{10}\log w = -30(0.2)25$ . We compare these results to those of S98 and find that not all data of S98 reach the claimed precision, with the worst deviation being larger than 7%. Most data points are in excellent agreement though. We then continued to produce a table of thermally averaged Gaunt factors covering the parameter space  ${}^{10}\log \gamma^2 = -6(0.2)10$  and  ${}^{10}\log u = -16(0.2)13$ , which is more than sufficient for the current needs of Cloudy. This table will be used in upcoming releases of Cloudy. A comparison of our data with S98 shows that most are in good agreement with a worst discrepancy of 0.13%. At this point we need to warn the reader that in several places in S98 the parameters of the Gaunt factor were transposed, most importantly in the electronic version of the table of thermally averaged Gaunt factors. Finally we produced a table of the frequency integrated Gaunt factor covering the parameter space  ${}^{10}\log \gamma^2 = -6(0.2)10$ . We find a small systematic offset between our data and those of S98, which is likely due to the omission of the part of the integral below  $u = 10^{-4}$  by S98. We present fits to the limiting behavior of this function, as well as rational function fits to the data in the table.

All data presented in this paper are available in electronic form from MNRAS as well as the Cloudy web site at <http://data.nublado.org/gauntff/>. In addition to these data tables, the Cloudy web site also presents simple interpolation routines written in Fortran and C. They use a 3rd-order Lagrange scheme to interpolate the linear Gaunt data. This reaches a relative precision better than  $1.5 \times 10^{-4}$  everywhere. The next release of Cloudy will contain a vectorized version of the interpolation routine which is faster, while



maintaining the same precision. It is based on the Newton interpolation technique. The supplied interpolation routines work both on the non-averaged and thermally averaged Gaunt factor tables. Separate programs are provided for interpolating the frequency integrated Gaunt factors based on the fits reported in this paper. The program used to calculate all data is also available from this web site.

## ACKNOWLEDGMENTS

PvH acknowledges support from the Belgian Science Policy Office through the ESA PRODEX program. GJF acknowledges support by NSF (1108928, 1109061, and 1412155), NASA (10-ATP10-0053, 10-ADAP10-0073, NNX12AH73G, and ATP13-0153), and STScI (HST-AR-13245, GO-12560, HST-GO-12309, and GO-13310.002-A). Our implementation of Spouge's algorithm for calculating the complex gamma function was based on the description on Wikipedia<sup>1</sup>

## REFERENCES

- Abramowitz M., Stegun I. A., 1972, Handbook of Mathematical Functions. Dover, New York
- Beckert T., Duschl W. J., Mezger P. G., 2000, A&A, 356, 1149
- Biedenharn L. C., 1956, Physical Review, 102, 262
- Ferland G. J., Porter R. L., van Hoof P. A. M., Williams R. J. R., Abel N. P., Lykins M. L., Shaw G., Henney W. J., Stancil P. C., 2013, Rev. Mex. Astron. Astrofis., 49, 137
- Gaunt J. A., 1930, Royal Society of London Philosophical Transactions Series A, 229, 163
- Hummer D. G., 1988, ApJ, 327, 477
- Karzas W. J., Latter R., 1961, ApJS, 6, 167 (KL61)
- Menzel D. H., Pekeris C. L., 1935, MNRAS, 96, 77 (MP35)
- Nozawa S., Itoh N., Kohyama Y., 1998, ApJ, 507, 530
- Press W. H., Teukolsky S. A., Vetterling W. T., Flannery B. P., 1992, Numerical recipes in C. The art of scientific computing, 2nd ed.. Cambridge University Press
- Spouge J. L., 1994, SIAM J. Numer. Anal., 31, 931
- Sutherland R. S., 1998, MNRAS, 300, 321 (S98)

<sup>1</sup> [http://en.wikipedia.org/wiki/Spouge's\\_approximation](http://en.wikipedia.org/wiki/Spouge's_approximation).

**APPENDIX A: A SERIES EXPANSION FOR THE FREE-FREE GAUNT FACTOR**

The procedure to derive a series expansion for the free-free Gaunt factor is described in great detail in the Appendix of MP35. Here we will discuss only those steps that need to be modified in order to correct the error in the series expansion and derive one additional term. All calculations were carried out with Maxima v5.31.3. First we need to extend Eq. A (9) from MP35 to include higher order terms and also correct a typo in the leftmost term:

$$-\tau/(1-\alpha^2) \equiv y^3 = \frac{u^3}{12\beta^3} + \frac{u^4}{8\beta^4} + \frac{(11+\alpha^2)u^5}{80\beta^5} + \frac{(13+3\alpha^2)u^6}{96\beta^6} + \frac{(57+22\alpha^2+\alpha^4)u^7}{448\beta^7} + \frac{(15+8\alpha^2+\alpha^4)u^8}{128\beta^8} \\ + \frac{(247+163\alpha^2+37\alpha^4+\alpha^6)u^9}{2304\beta^9} + \frac{(251+191\alpha^2+65\alpha^4+5\alpha^6)u^{10}}{2560\beta^{10}} + O(u^{11}). \quad (\text{A1})$$

Next we need to evaluate the integrals  $P$  and  $Q$  defined in Eqs. A (20) and A (21) of MP35, for which we need the quantities

$$q = [(1-x-z)/(z+\beta)^2]_A^B = [(\beta+\beta^2-u)/u^2]_A^B \quad (\text{A2})$$

and

$$p = [(z-z^2)/(z+\beta)^2]_A^B = [\{(2u-1)\beta-\beta^2+u-u^2\}/u^2]_A^B, \quad (\text{A3})$$

where we used the identities  $x = 1 - \beta^2$  and  $z \equiv u - \beta$ . We can invert Eq. A1 to derive a Taylor expansion of  $u(y)$  and substitute that into Eqs. A2 and A3. This yields

$$\frac{q}{p} = \left[ + \frac{\beta+1}{12^{2/3}\beta y^2} + \frac{1}{12^{1/3}y} - \frac{2\alpha^2(\beta+1)+7\beta-3}{20\beta} + \frac{12^{1/3}(1+\alpha^2)y}{20} - \frac{12^{2/3}(\beta+1)(3-4\alpha^2+3\alpha^4)y^2}{560\beta} \right. \\ \left. + \frac{(12-51\alpha^2+12\alpha^4)y^3}{700} \pm \frac{12^{1/3}(\beta+1)(1-2\alpha^2-2\alpha^4+\alpha^6)y^4}{600\beta} - \frac{12^{2/3}(1-47\alpha^2-47\alpha^4+\alpha^6)y^5}{42000} \pm O(y^6) \right]_A^B, \quad (\text{A4})$$

where the upper sign pertains to  $q$  and the lower sign to  $p$ . Here we can see that the  $y^2$  term differs from what is stated in MP35. At B we have  $y = e^{i5\pi/6} \left| \frac{\tau}{1-\alpha^2} \right|^{1/3}$ , and at A we have  $y = e^{i\pi/6} \left| \frac{\tau}{1-\alpha^2} \right|^{1/3}$ . Substituting these values in Eq. A4 and carrying out the integration yields

$$\frac{Q}{P} \approx -\frac{e^{\pi\eta_f}\beta^{-i(\eta_i+\eta_f)}\sqrt{3}}{2\pi} \left( + i \frac{(\beta+1)(1-\alpha^2)^{2/3}\Gamma(1/3)}{12^{2/3}\beta\eta_f^{1/3}} - \frac{(1-\alpha^2)^{1/3}\Gamma(2/3)}{12^{1/3}\eta_f^{2/3}} - \frac{12^{1/3}(1+\alpha^2)\Gamma(1/3)}{60(1-\alpha^2)^{1/3}\eta_f^{4/3}} \right. \\ \left. + i \frac{12^{2/3}(\beta+1)(3-4\alpha^2+3\alpha^4)\Gamma(2/3)}{840(1-\alpha^2)^{2/3}\beta\eta_f^{5/3}} + i \frac{2(\beta+1)(1-2\alpha^2-2\alpha^4+\alpha^6)\Gamma(1/3)}{225 \cdot 12^{2/3}(1-\alpha^2)^{4/3}\beta\eta_f^{7/3}} \right. \\ \left. - \frac{(1-47\alpha^2-47\alpha^4+\alpha^6)\Gamma(2/3)}{3150 \cdot 12^{1/3}(1-\alpha^2)^{5/3}\eta_f^{8/3}} + O\left[(1-\alpha^2)^{-7/3}\eta_f^{-10/3}\right] \right) \quad (\text{A5})$$

where we used the same sign convention as before. Here we replaced the upper limit  $2\pi$  of the integral with  $\infty$ . This is well justified since  $\eta_f > 907$  everywhere in the region where we use the series expansion, implying that the contribution from  $\tau = 2\pi$  to  $\infty$  to the integral is vanishingly small due to the  $e^{-\eta_f\tau}$  term in the integrand.

Having obtained these results, we can now find expressions for the hypergeometric functions using

$${}_2F_1(1-i\eta_f, -i\eta_i; 1; x) = \beta^{2i(\eta_i+\eta_f)}Q, \quad \text{and} \quad {}_2F_1(1-i\eta_i, -i\eta_f; 1; x) = \beta^{2i(\eta_i+\eta_f)}P.$$

Hence with

$$\Delta \equiv {}_2F_1^2(1-i\eta_f, -i\eta_i; 1; x) - {}_2F_1^2(1-i\eta_i, -i\eta_f; 1; x) = \beta^{4i(\eta_i+\eta_f)}(Q^2 - P^2)$$

we can now derive the series expansion for the Gaunt factor from

$$g_{\text{ff}} = \frac{\pi\sqrt{3}\eta_i\eta_f e^{-2\pi\eta_f} |\Delta|}{(\eta_i-\eta_f)(1-e^{-2\pi\eta_i})(1-e^{-2\pi\eta_f})} \approx 1 + \frac{\Gamma(1/3)(1+\alpha^2)}{5 \cdot 12^{1/3}\Gamma(2/3)(1-\alpha^2)^{2/3}\eta_f^{2/3}} - \frac{6\Gamma(2/3)(3-4\alpha^2+3\alpha^4)}{35 \cdot 12^{2/3}\Gamma(1/3)(1-\alpha^2)^{4/3}\eta_f^{4/3}} \\ - \frac{(3-\alpha^2-\alpha^4+3\alpha^6)}{175(1-\alpha^2)^{6/3}\eta_f^{6/3}} + O\left[(1-\alpha^2)^{-8/3}\eta_f^{-8/3}\right], \quad (\text{A6})$$

where we used the identities  $(1-\alpha^2)(\beta+1)/\beta = 2(\eta_i-\eta_f)/\eta_i$  and  $\Gamma(1/3)\Gamma(2/3) = 2\pi/\sqrt{3}$ . We also approximated the terms  $1 - e^{-2\pi\eta_i} \approx 1$  and  $1 - e^{-2\pi\eta_f} \approx 1$ . The latter assumptions are again well justified as  $\eta_i \geq 1000$  and  $\eta_f > 907$  everywhere in the region where we use the series expansion.